Fluctuations of Pigment's Dipole Moment Orientations in B850 Ring from Photosynthetic Complex LH2

PAVEL HEŘMAN
Univ. of Hradec Králové
Faculty of Science
Department of Physics
Rokitanského 62
Hradec Králové
CZECH REPUBLIC
pavel.herman@uhk.cz

DAVID ZAPLETAL
University of Pardubice
Faculty of Econ. and Admin.
Inst. of Mathematics
and Quant. Methods
Studentská 95, Pardubice
CZECH REPUBLIC
david.zapletal@upce.cz

JAN LOSKOT
Univ. of Hradec Králové
Faculty of Science
Department of Physics
Rokitanského 62
Hradec Králové
CZECH REPUBLIC
loskoja1@uhk.cz

ANDREA HLADÍKOVÁ
Univ. of Hradec Králové
Faculty of Science
Department of Physics
Rokitanského 62
Hradec Králové
CZECH REPUBLIC
hladian2@uhk.cz

Abstract: Properties of light–harvesting (LH) pigment–protein complexes are strongly influenced by interactions with environment. Some of these interactions could be modeled by different types of static disorder. Slow fluctuations of bacteriochlorophyll's dipole moment orientations represent one possible type of static disorder in B850 ring from LH2 complex of purple bacteria. This type of static disorder is investigated in present paper. Two modifications of such uncorrelated static disorder type (Gaussian fluctuations of dipole moment orientations in the ring plane and Gaussian fluctuations of dipole moment orientations in a plane which is perpendicular to the ring one) are taking into account. The nearest neighbour transfer integral distributions for different strengths of static disorder are presented and the most important statistical properties are calculated, discussed and compared.

Key–Words: LH2 complex, B850 ring, static disorder, Hamiltonian, transfer integral distributions

1 Introduction

Some organisms, e.g. green plants, bacteria, blue–green algae, etc., have ability to transform energy of light into chemical energy. This process is called photosynthesis. Photosynthesis could be divided to two stages (light stage and dark stage). The first (light) stage consists of photochemical reactions. Light photon is absorbed in this first stage and a series of electron transfers is driven by its energy. As the result, adenosine triphosphate (ATP) and nicotine adenine dinucleotide phosphate (NADPH – reduced form) are synthesized. The ATP and NADPH formed in the light–capturing reactions are used for reduction of carbon dioxide to organic carbon compounds during the second (dark) stage [1].

Researchers have been focused on investigation of photosynthesis for a long time. Our research is concerned the light stage of photosynthesis in purple bacteria. Absorption of solar photons by a complex system of membrane–associated pigment–proteins (light–harvesting (LH) antenna) gives excitation energy (in the form of Frenkel excitons). Then efficient transfer to a reaction center occurs. There excitons are converted into a chemical energy [2].

Geometric structures of photosynthetic complexes from purple bacteria are known in great detail from X–ray crystallography. Their antenna systems (LH1, LH2, LH3, and LH4) are arranged as ring units. A ring–shaped structure is formed by cyclic repetition of identical subunits. The organization of these light–harvesting complexes is generally the same, but their symmetry can be different.

Crystal structure of peripheral LH2 complex contained in purple bacterium *Rhodopseudomonas acidophila* was described first (McDermott et al. [3] and then further e.g. Papiz et al. [4]). Two concentric rings (B850 ring and B800 one) are created by bacteriochlorophyll (BChl) molecules. Eighteen closely packed BChl molecules are arranged in B850 ring (with absorption band at about 850 nm). B800 ring consists of nine well–separated BChl molecules absorbing around 800 nm. Organization of the whole LH2 complex is nonameric, i.e. it consists of nine identical subunits. Dipole moments of BChl molecules in LH2 complex are oriented approximately tangentially to the ring. Arrangement of LH2 complexes from other purple bacteria is analogous.

Other types of peripheral light–harvesting complexes can be also found in some purple bacteria (B800–820 LH3 complex in *Rhodopseudomonas acidophila* strain 7050 or LH4 complex in *Rhodopseudomonas palustris*). LH3 complex like LH2 one is usually nonameric [5]. LH4 complex consists of eight identical subunits, i.e. it is octameric, and it con-

sists of three concentric BChl rings [6]. Light harvesting complexes can also differ in orientations of BChl dipole moments and consequently in strengths of mutual interactions between BChl molecules. For instance, BChl dipole moments in B−α/B−β ring from LH4 complex are oriented approximately radially to the ring. Interactions between the nearest neighbour bacteriochlorophylls in B−α/B−β ring are approximately two times weaker in comparison with B850 ring from LH2 complex and they have opposite sign.

Purple bacteria contain (beside peripheral antenna complexes) also core antenna complexes that include reaction centers. For instance LH1 complex from *Rhodopseudomonas acidophila* or *Rhodopseudomonas palustris* consists of approximately 16 structural subunits in which two bacteriochlorophyll molecules are noncovalently attached to pairs of transmembrane polypeptides. These subunits again have ringlike structure which surrounds reaction center [7].

The intermolecular distances under 1 nm imply strong exciton couplings between corresponding BChl molecules. Therefore an extended Frenkel exciton states model can be applied in theoretical approach. The solvent and protein environment of bacteriochlorophyll rings fluctuates. Characteristic time scale of these fluctuations at room temperature have range from femtoseconds to nanoseconds. Fast fluctuations can be modeled by dynamic disorder and slow fluctuations by static disorder. Influence of static disorder in local excitation energies on the anisotropy of fluorescence for LH2 complexes was studies by Kumble and Hochstrasser [8] and Nagarajan et al. [9, 10]. We extended these investigations by addition of dynamic disorder. This effect was studied by us for simple model systems [11–13] and then for models of B850 ring (from LH2) [14, 15]. We also consider various types of uncorrelated static disorder and correlated one (e.g., elliptical deformation) [16–18]. Comparison of the results for B850 ring from LH2 complex and B−α/B−β ring from LH4 complex, that have different arrangements of optical dipole moments, was also done [19–22]. Recently, our investigation has been focused on the modeling of absorption and fluorescence spectra of LH2 and LH4 complexes within the nearest neighbour approximation model [23–27] and full Hamiltonian model [28–36].

Very recently we have started to investigate the nearest neighbour transfer integral distributions for various types of static disorder connected with fluctuations in ring geometry. Main goal of the present paper is the investigation of transfer integral distributions for fluctuations of BChl dipole moment orientations in B850 ring from LH2 complex. The rest of the paper is structured as follows. Section 2 introduces the ring model with different types of static disorder.

Used units and parameters can be found in Section 3. Results are presented and discussed in Section 4 and conclusions are drawn in Section 5.

2 Model

We consider only one exciton on molecular ring, e.g. B850 ring from LH2 complex. Then Hamiltonian of the exciton consists of four terms in our model:

$$H = H_{\text{ex}}^0 + H_{\text{s}} + H_{\text{ph}} + H_{\text{ex}-\text{ph}}. \quad (1)$$

2.1 Ideal ring

The first term in Eq. (1),

$$H_{\text{ex}}^0 = \sum_{m=1}^{N} E_m^0 a_m^\dagger a_m + \sum_{m,n=1(m\neq n)}^{N} J_{mn}^0 a_m^\dagger a_n, \quad (2)$$

describes an exciton on the ideal ring, i.e. without any disorder. Here $a_m^\dagger$ (a_m) are creation (annihilation) operators of the exciton at site m, E_m^0 is the local excitation energy of m–th molecule, J_{mn}^0 (for $m \neq n$) is the so–called transfer integral between sites m and n. N is the number of molecules in the ring ($N = 18$ for B850 ring from LH2 complex). Local excitation energies E_m^0 are the same for all bacteriochlorophylls on unperturbed ring, i.e.

$$E_m^0 = E_0, \quad m = 1, \ldots, N.$$

The interaction strengths between the nearest neighbour bacteriochlorophylls inside one subunit and between subunits are almost the same in B850 ring from LH2 complex (see Figure 1 (B) in [6]). That is why such ring can be modeled as homogeneous case,

$$J_{mn}^0 = J_{m+i,n+i}^0. \quad (3)$$

Transfer integrals J_{mn} in dipole–dipole approximation read

$$J_{mn} = \frac{\vec{d}_m \cdot \vec{d}_n}{|\vec{r}_{mn}|^3} - 3\frac{\left(\vec{d}_m \cdot \vec{r}_{mn}\right)\left(\vec{d}_n \cdot \vec{r}_{mn}\right)}{|\vec{r}_{mn}|^5} =$$

$$= |\vec{d}_m||\vec{d}_n|\frac{\cos\varphi_{mn} - 3\cos\varphi_m \cos\varphi_n}{|\vec{r}_{mn}|^3}. \quad (4)$$

Local dipole moments of m–th and n–th molecule are denoted as $\vec{d}_m$ and $\vec{d}_n$, the angle between these dipole moment vectors ($\vec{d}_m$, $\vec{d}_n$) is referred to as φ_{mn}. $\vec{r}_{mn}$ represents the vector connecting m–th and n–th molecule, φ_m (φ_n) symbolizes the angle between $\vec{d}_m$

$(\vec{d}_n)$ and $\vec{r}_{mn}$. In case of ideal ring (without any disorder) we consider the same distances $r_{m,m+1}$ of neighbouring bacteriochlorophyll molecules. Therefore angles $\beta_{m,m+1}$ have to be the same too ($\beta_{m,m+1} = 2\pi/18$, see Figure 1). The reason for this is the requirement of correspondence between the geometric arrangement of B850 ring and interaction strengths between the nearest neighbour bacteriochlorophylls.
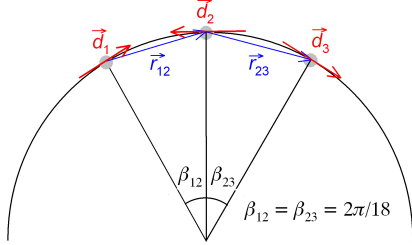

Figure 1: Geometric arrangement of ideal B850 ring from LH2 complex (without any fluctuations – dipole moments are oriented tangentially to the ring)

In what follows we consider that only the nearest neighbour transfer matrix elements are nonzero, i.e. the nearest neighbour approximation model. In this case we have

$$J_{mn}^0 = J_0(\delta_{m,n+1} + \delta_{m,n-1}). \qquad (5)$$

The wave vector representation with corresponding delocalized Bloch states α and energies E_α can be used for diagonalization of the pure exciton Hamiltonian H_{ex}^0. Then H_{ex}^0 reads

$$H_{\text{ex}}^0 = \sum_{\alpha=1}^{N} E_\alpha a_\alpha^\dagger a_\alpha, \qquad (6)$$

with a_α (Fourier transformed excitonic operator in α–representation). Considering homogeneous case and the nearest neighbour approximation model, the operators a_α and the energies E_α from Eq. (6) have the form

$$a_\alpha = \sum_{n=1}^{N} a_n e^{i\alpha n}, \ \alpha = \frac{2\pi}{N}l, \ l = 0, \dots, \pm\frac{N}{2}, \quad (7)$$

$$E_\alpha = E_0 - 2J_0 \cos\alpha. \qquad (8)$$

2.2 Static disorder

The second term in Eq. 1, H_s, corresponds to static disorder. One of the ways to take into account such disorder is to model it as slow fluctuations in ring geometry. Deviation in ring geometry results in changes of transfer integrals δJ_{mn} ($m \neq n$),

$$J_{mn} = J_{nm} = J_{mn}^0 + \delta J_{mn}. \qquad (9)$$

Static disorder in ring geometry can be consider in two ways – fluctuations in molecular positions or fluctuations in molecular dipole moment orientations. We studied first type of fluctuations as only in the ideal ring plane [37] as out of the ideal ring plane [38]. In the present paper we investigate the second type, i.e. deviations of molecular dipole moment orientations.

The simplest possibility is to neglect the changes of dipole moment orientations out of the ring plane. Then we have:

a) uncorrelated fluctuations of molecular dipole moment orientations $\delta\theta_m$ in the plane of ideal ring (Gaussian distribution and standard deviation Δ_θ),

$$\theta_m = \theta_m^0 + \delta\theta_m, \qquad (10)$$

where θ_m^0 characterizes the dipole moment direction of m–the molecule in the ideal ring (see Figure 2).
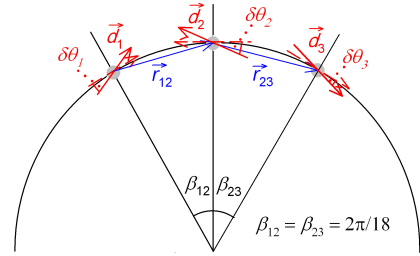

Figure 2: B850 ring from LH2 complex – fluctuations in bacteriochlorophyll dipole moment orientations $\delta\theta_m$ in the ideal ring plane

If the dipole moment orientations are changed out of the ideal ring plane, we get:

b) uncorrelated fluctuations of molecular dipole moment orientations $\delta\gamma_m$ – fluctuations occur only in the plane which is perpendicular to the ideal ring one (Gaussian distribution and standard deviation Δ_γ),

$$\gamma_m = \delta\gamma_m. \qquad (11)$$

Here γ_m determines the angle between m–th dipole moment vector and the plane of the ideal ring. (see Figure 3).

Due to the consideration of dipole–dipole approximation the connection between disorder in geometric arrangement and in transfer integrals is given by Eq. (4).

Finally, the third and fourth term in Eq (1), H_{ph} and $H_{\text{ex–ph}}$, represents dynamic disorder, i.e. phonon bath and exciton–phonon interaction. We consider only static disorder and neglect these terms in this paper.
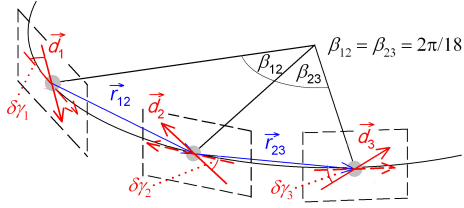
Figure 3: B850 ring from LH2 complex – fluctuations in bacteriochlorophyll dipole moment orientations $\delta\gamma_m$ in the plane which is perpendicular to the ideal ring one

3   Units and Parameters

Dimensionless energies normalized to the transfer integral $J_{m,m+1} = J_0$ (see Eq. (5)) have been used in our calculations. Estimation of J_0 varies in literature between 250 cm^{-1} and 400 cm^{-1}.

In our previous investigations [39] we found from comparison with experimental results for B850 ring from the LH2 complex [40] that the possible strength Δ_J of the uncorrelated Gaussian static disorder in transfer integrals δJ_{mn} is approximately $\Delta_J \approx 0.15\, J_0$. The strengths of above mentioned types of static disorder in ring geometry is taken in connection with the strength Δ_J. That is why for our types of static disorder we have taken the strengths in following intervals:

a) uncorrelated fluctuations of molecular dipole moment orientations $\delta\theta_m$ in the plane of ideal ring $\Delta_\theta \in \langle 0.02\, \pi, 0.20\, \pi\rangle$,

b) uncorrelated fluctuations of molecular dipole moment orientations $\delta\gamma_m$ only in the plane which is perpendicular to the ideal ring one $\Delta_\gamma \in \langle 0.02\, \pi, 0.20\, \pi\rangle$,

In both cases calculations were done for 10000 realizations of static disorder.

4   Results and Discussion

Static disorder connected with fluctuations in ring geometry, namely fluctuations in molecular dipole moment orientations, is investigated in present paper. These fluctuations strongly influence Hamiltonian of B850 ring from LH2 complex. Distributions of the nearest neighbour transfer integrals $J_{m,m+1}$ were calculated for above mentioned three modifications of this static disorder type. Graphical presentation of these distributions is done by contour

plots and by line plots. Values of $E(J_{m,m+1})$ and $E(J_{m,m+1}) \pm \sqrt{D(J_{m,m+1})}$ are also included in contour plots. Here $E(J_{m,m+1})$ is sample expected value,

$$E(J_{m,m+1}) = \frac{1}{n}\sum_{i=1}^{n} J_{m,m+1}, \qquad (12)$$

and $\sqrt{D(J_{m,m+1})}$ is sample standard deviation,

$$\sqrt{D(J_{m,m+1})} = \sqrt{\frac{1}{(n-1)}M_2}. \qquad (13)$$

In addition, sample skewness α_3,

$$\alpha_3 = \frac{n^{\frac{5}{2}}}{(n-1)(n-2)}\frac{M_3}{M_2^{\frac{3}{2}}}, \qquad (14)$$

and sample kurtosis α_4,

$$\alpha_4 = \frac{n^2}{(n-2)(n-3)}\left[\frac{n(n+1)}{n-1}\frac{M_4}{M_2^2} - 3\right], \quad (15)$$

are calculated. Here M_k, which is given by

$$M_k = \sum_{i=1}^{n}\left[J_{m,m+1} - E(J_{m,m+1})\right]^k, \qquad (16)$$

denotes k–th central moment of $J_{m,m+1}$ and n is the number of cases in our samples. Our results were calculated from 10000 realizations of static disorder and due to dimension of Hamiltonian ($N = 18$) the number of cases n equals 180000. Also sample coefficient of variation c was calculated,

$$c = \frac{\sqrt{D(J_{m,m+1})}}{E(J_{m,m+1})}. \qquad (17)$$

Both modifications of fluctuations in molecular dipole moment orientations were compared in detail by this coefficient.

Distributions of the nearest neighbour transfer integrals $J_{m,m+1}$ for above mentioned types of static disorder are presented in Figure 4 and Figure 5. Distributions of $J_{m,m+1}$ for Gaussian uncorrelated fluctuations $\delta\theta_m$ of molecular dipole moment orientations in the plane of ideal ring are drawn in Figure 4. Figure 5 shows the distributions of $J_{m,m+1}$ for Gaussian uncorrelated fluctuations $\delta\gamma_m$ of molecular dipole moment orientations in the plane which is perpendicular to the ideal ring one.

Dependencies of $E(J_{m,m+1})$ and $\sqrt{D(J_{m,m+1})}$ on corresponding static disorder strength are also presented in Figure 4 – left column ($\delta\theta_m$) and Figure 5
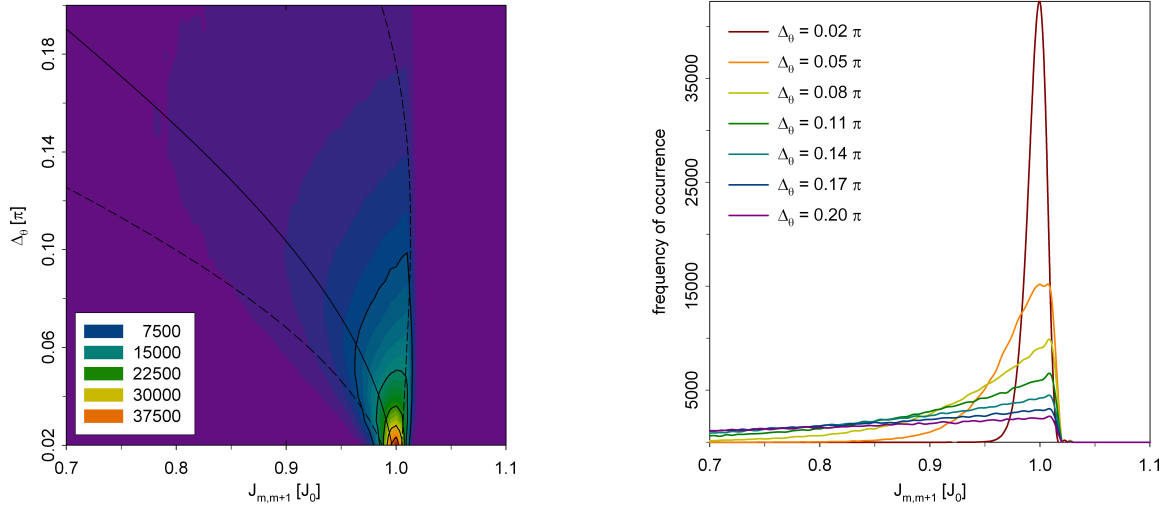
Figure 4: Distributions of the nearest neighbour transfer integrals $J_{m,m+1}$ for B850 ring from LH2 complex – uncorrelated Gaussian fluctuations $\delta\theta_m$ in molecular dipole moment directions in the plane of ideal ring; standard deviation (the strength of static disorder) $\Delta_\theta \in \langle 0.02\,\pi, 0.20\,\pi \rangle$

Δ_θ	expected value $E(J_{m,m+1})$	standard deviation $\sqrt{D(J_{m,m+1})}$	skewness α_3	kurtosis α_4	coefficient of variation c
$0.02\,\pi$	$0.996\,J_0$	$0.009\,J_0$	-0.787	0.999	0.009
$0.05\,\pi$	$0.976\,J_0$	$0.033\,J_0$	-1.684	4.613	0.034
$0.08\,\pi$	$0.939\,J_0$	$0.073\,J_0$	-1.954	5.827	0.078
$0.11\,\pi$	$0.888\,J_0$	$0.126\,J_0$	-1.941	5.353	0.141
$0.14\,\pi$	$0.824\,J_0$	$0.186\,J_0$	-1.811	4.261	0.226
$0.17\,\pi$	$0.752\,J_0$	$0.250\,J_0$	-1.629	3.057	0.332
$0.20\,\pi$	$0.674\,J_0$	$0.312\,J_0$	-1.428	1.965	0.463

Table 1: Expected value, standard deviation, skewness, kurtosis and coefficient of variation for the nearest neighbour transfer integral $J_{m,m+1}$ distributions of uncorrelated Gaussian fluctuations of molecular dipole moment orientations $\delta\theta_m$ in the plane of ideal ring (seven strengths Δ_θ)

– left column ($\delta\gamma_m$). Additionally, Table 1 and Table 2 contain the values of sample characteristics $E(J_{m,m+1})$, $\sqrt{D(J_{m,m+1})}$, α_3, α_4 and c (see Eq. (12) – Eq. (17)) for chosen static disorder strengths.

At the present paper we focus only on the types of static disorder connected with deviations in molecular dipole moment orientations ($\delta\theta_m$ and $\delta\gamma_m$. If we consider Gaussian distribution of molecular dipole moment orientations, resulting distributions of the nearest neighbour transfer integrals $J_{m,m+1}$ are non–Gaussian. From Figures 4, 5 and Tables 1, 2 it is clear that the expected value $E(J_{m,m+1})$ is non–constant and standard deviation $\sqrt{D(J_{m,m+1})}$ depends on static disorder strength for both static disor-

der types. On the other hand, Gaussian distribution of transfer integrals $J_{m,m+1}$ has constant expected value, i.e. $E(J_{m,m+1}) = J_0$, and standard deviation equals the strength of static disorder $\sqrt{D(J_{m,m+1})} = \Delta_J$. Level of deviation from Gaussian distribution can also be assessed through skewness α_3 and kurtosis α_4. These characteristics are nonconstant for both static disorder types connected with fluctuations in molecular dipole moment orientations (contrary, $\alpha_3 = \alpha_4 = 0$ for Gaussian distribution). As concerns expected value $E(J_{m,m+1})$, we can see decrease of it for increasing static disorder strength in both cases of fluctuations ($\delta\theta_m$ and $\delta\gamma_m$) Values of $E(J_{m,m+1})$ are practically the same for both types of static disorder.
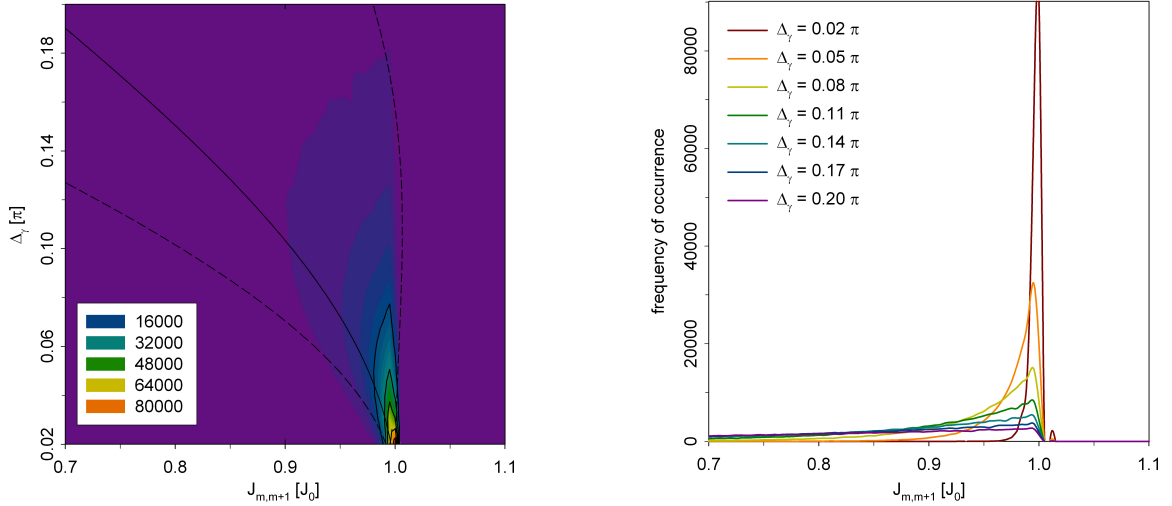
Figure 5: Distributions of the nearest neighbour transfer integrals $J_{m,m+1}$ for B850 ring from LH2 complex – uncorrelated Gaussian fluctuations $\delta\gamma_m$ of molecular dipole moment orientations only in the plane which is perpendicular to the ideal ring one; standard deviation (the strength of static disorder) $\Delta_\gamma \in \langle 0.02\,\pi, 0.20\,\pi \rangle$

Δ_γ	expected value $E(J_{m,m+1})$	standard deviation $\sqrt{D(J_{m,m+1})}$	skewness α_3	kurtosis α_4	coefficient of variation c
$0.02\,\pi$	$0.996\,J_0$	$0.004\,J_0$	-2.493	9.610	0.004
$0.05\,\pi$	$0.976\,J_0$	$0.027\,J_0$	-2.419	8.879	0.028
$0.08\,\pi$	$0.939\,J_0$	$0.066\,J_0$	-2.288	7.666	0.071
$0.11\,\pi$	$0.888\,J_0$	$0.119\,J_0$	-2.113	6.182	0.134
$0.14\,\pi$	$0.824\,J_0$	$0.180\,J_0$	-1.907	4.646	0.218
$0.17\,\pi$	$0.752\,J_0$	$0.244\,J_0$	-1.685	3.231	0.324
$0.20\,\pi$	$0.674\,J_0$	$0.306\,J_0$	-1.462	2.034	0.454

Table 2: Expected value, standard deviation, skewness, kurtosis and coefficient of variation for the nearest neighbour transfer integral $J_{m,m+1}$ distributions of uncorrelated Gaussian fluctuations $\delta\gamma_m$ of molecular dipole moment orientations only in the plane which is perpendicular to the ideal ring one (seven strengths Δ_γ)

For standard deviation $\sqrt{D(J_{m,m+1})}$ the dependencies of it on static disorder strength are very similar in case of $\delta\theta_m$ and $\delta\gamma_m$. They are nonlinear for small static disorder strengths ($\Delta \in \langle 0.02\,\pi, 0.10\,\pi \rangle$) and they become approximately linear for higher values of Δ.

The distributions of $J_{m,m+1}$ are negatively skewed (to the left hand side) for both static disorder types (see Figure 4 and Figure 5, right columns). It corresponds with negative values of sample skewness (see Table 1 and Table 2). All these distributions have also higher sample kurtosis α_4 in comparison with Gaussian distribution of $J_{m,m+1}$. In case of $\delta\theta_m$ the dependence of α_4 have maximum approximately in the middle of our interval of Δ_θ. Contrary, In case of $\delta\gamma_m$ the dependence of α_4 on Δ_γ is monotonous. The value of α_4 is highest for the lowest value of Δ_γ. Due to non-constant expected value, influences of different types of fluctuations to distribution of $J_{m,m+1}$ can be compared using the coefficient of variation c. Our previous investigations [39] led to suitable strength of static disorder in transfer integrals $\Delta_J \approx 0.15\,J_0$ and consequently $c \approx 0.15$. As concerns fluctuations in molecular dipole moment orientations, approximately same value of coefficient of variation corresponds to the following disorder strengths: $\Delta_\theta \approx 0.11 - 0.12\,\pi$ and $\Delta_\gamma \approx 0.12\pi$.
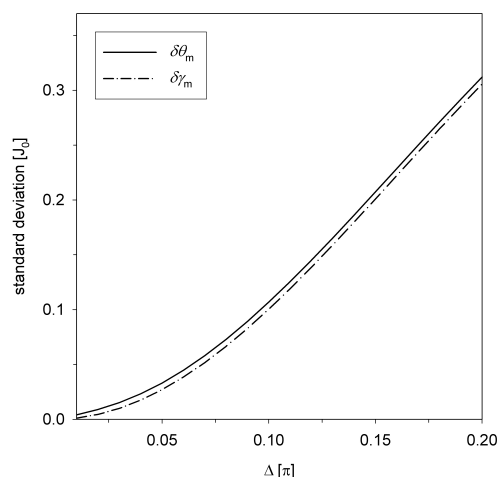
Pavel Herman, David Zapletal,
Jan Loskot, Andrea Hladikova

Figure 6: Dependence of standard deviations $\sqrt{D(J_{m,m+1})}$ on static disorder strength Δ for two types of fluctuations $\delta\theta_m$ and $\delta\gamma_m$

5 Conclusions

Comparison of the results obtained within different types of static disorder connected with fluctuations in molecular dipole moment orientations can be summarized as follows. Expected value of the nearest neighbour transfer integral distribution depends on static disorder strength and the dependences are practically the same for both presented types of fluctuations. The dependence of standard deviation on the static disorder strength shows the nonlinearity as for fluctuations $\delta\theta_m$ as for $\delta\gamma_m$. For both types of static disorder the distributions of $J_{m,m+1}$ are significantly skewed and have nonzero kurtosis. Through the comparison of coefficient of variation c we are able to estimate suitable strength of static disorder connected with fluctuations in molecular dipole moment orientations.

References:

[1] D. W. Lawlor, *Photosynthesis*, Spriger, New York 2001.

[2] R. van Grondelle and V. I. Novoderezhkin, Energy transfer in photosynthesis: experimental insights and quantitative models, *Phys. Chem. Chem. Phys.* 8, 2003, pp. 793–807.

[3] G. McDermott, et al., Crystal structure of an integral membrane light-harvesting complex from photosynthetic bacteria, *Nature* 374, 1995, pp. 517–521.

[4] M. Z. Papiz, et al., The structure and thermal motion of the B 800-B850 LH2 complex from Rps. acidophila at 2.0 A resolution and 100 K: new structural features and functionally relevant motions, *J. Mol. Biol.* 326, 2003, pp. 1523–1538.

[5] K. McLuskey, et al., The crystalographic structure of the B800–820 LH3 light-harvesting complex from the purple bacteria Rhodopseudomonas acidophila strain 7050, *Biochemistry* 40, 2001, pp. 8783–8789.

[6] W. P. F. de Ruijter, et al., Observation of the Energy–Level Structure of the Low–Light Adapted B800 LH4 Complex by Single–Molecule Spectroscopy, *Biophys. J.* 87, 2004, pp. 3413–3420.

[7] A. W. Roszak, et al., Crystal structure of the RC-LH1 core complex from Rhodopseudomonas palustris, *Science* 302, 2003, pp. 1976–1972.

[8] R. Kumble and R. Hochstrasser, Disorder–induced exciton scattering in the light–harvesting systems of purple bacteria: Influence on the anisotropy of emission and band $\rightarrow$ band transitions, *J. Chem. Phys.* 109, 1998, pp. 855–865.

[9] V. Nagarajan, et al., Femtosecond pump–probe spectroscopy of the B850 antenna complex of Rhodobacter sphaeroides at room temperature, *J. Phys. Chem. B* 103, 1999, pp. 2297–2309.

[10] V. Nagarajan and W. W. Parson, Femtosecond fluorescence depletion anisotropy: Application to the B850 antenna complex of Rhodobacter sphaeroides, *J. Phys. Chem. B* 104, 2000, pp. 4010–4013.

[11] V. Čápek, I. Barvík and P. Heřman, Towards proper parametrization in the exciton transfer and relaxation problem: dimer, *Chem. Phys.* 270, 2001, pp. 141–156.

[12] P. Heřman and I. Barvík, Towards proper parametrization in the exciton transfer and relaxation problem. II. Trimer, *Chem. Phys.* 274, 2001, pp. 199–217.

[13] P. Heřman, I. Barvík and M. Urbanec, Energy relaxation and transfer in excitonic trimer, *J. Lumin.* 108, 2004, pp. 85–89.

[14] P. Heřman, et al., Exciton scattering in light–harvesting systems of purple bacteria, *J. Lumin.* 94–95, 2001, pp. 447–450.

[15] P. Heřman and I. Barvík, Non–Markovian effects in the anisotropy of emission in the ring antenna subunits of purple bacteria photosynthetic systems, *Czech. J. Phys.* 53, 2003, pp. 579–605.

[16] P. Heřman, et al., Influence of static and dynamic disorder on the anisotropy of emission in the ring antenna subunits of purple bacteria photosynthetic systems, *Chem. Phys.* 275, 2002, pp. 1–13.

[17] P. Heřman and I. Barvík, Temperature dependence of the anisotropy of fluorescence in ring molecular systems, *J. Lumin.* 122–123, 2007, pp. 558–561.

[18] P. Heřman, D. Zapletal and I. Barvík, Computer simulation of the anisotropy of fluorescence in ring molecular systems: Influence of disorder and ellipticity, *Proc. IEEE 12th Int. Conf. on Computational Science and Engineering*, Vancouver: IEEE Comp. Soc., 2009, pp. 437–442.

[19] P. Heřman and I. Barvík, Coherence effects in ring molecular systems, *Phys. Stat. Sol. C* 3, 2006, 3408–3413.

[20] P. Heřman, D. Zapletal and I. Barvík, The anisotropy of fluorescence in ring units III: Tangential versus radial dipole arrangement, *J. Lumin.* 128, 2008, pp. 768–770.

[21] P. Heřman, I. Barvík and D. Zapletal, Computer simulation of the anisotropy of fluorescence in ring molecular systems: Tangential vs. radial dipole arrangement, *Lecture Notes in Computer Science* 5101, 2008, pp. 661–670.

[22] P. Heřman, D. Zapletal and I. Barvík, Lost of coherence due to disorder in molecular rings, *Phys. Stat. Sol. C* 6, 2009, pp. 89–92.

[23] P. Heřman, D. Zapletal and J. Šlégr, Comparison of emission spectra of single LH2 complex for different types of disorder, *Phys. Proc.* 13, 2011, pp. 14–17.

[24] D. Zapletal and P. Heřman, Simulation of molecular ring emission spectra: localization of exciton states and dynamics, *Int. J. Math. Comp. Sim.* 6, 2012, pp. 144–152.

[25] M. Horák, P. Heřman and D. Zapletal, Simulation of molecular ring emission spectra – LH4 complex: localization of exciton states and dynamics, *Int. J. Math. Comp. Sim.* 7, 2013, pp. 85–93.

[26] P. Heřman and D. Zapletal, Intermolecular coupling fluctuation effect on absorption and emission spectra for LH4 ring, *Int. J. Math. Comp. Sim.* 7, 2013, pp. 249–257.

[27] M. Horák, P. Heřman and D. Zapletal, Modeling of emission spectra for molecular rings – LH2, LH4 complexes, *Phys. Proc.* 44, 2013, pp. 10–18.

[28] P. Heřman, D. Zapletal and M. Horák, Emission spectra of LH2 complex: full Hamiltonian model, *Eur. Phys. J. B* 86, 2013, art. no. 215.

[29] P. Heřman and D. Zapletal, Emission Spectra of LH4 Complex: Full Hamiltonian Model, *Int. J. Math. Comp. Sim.* 7, 2013, pp. 448–455.

[30] P. Heřman and D. Zapletal, Simulation of Emission Spectra for LH4 Ring: Intermolecular Coupling Fluctuation Effect, *Int. J. Math. Comp. Sim.* 8, 2014, pp. 73–81.

[31] D. Zapletal and P. Heřman, Photosynthetic complex LH2 – Absorption and steady state fluorescence spectra, *Energy* 77, 2014, pp. 212–219.

[32] P. Heřman and D. Zapletal, Simulations of emission spectra for LH4 Ring – Fluctuations in radial positions of molecules, *Int. J. Biol. Biomed. Eng.* 9, 2015, pp. 65–74.

[33] P. Heřman and D. Zapletal, Computer simulation of emission and absorption spectra for LH2 ring, *LNEE* 343, 2015, pp. 221–234.

[34] P. Heřman and D. Zapletal, Modeling of Absorption and Steady State Fluorescence Spectra of Full LH2 Complex (B850 – B800 Ring), *Int. J. Math. Mod. Meth. Appl. Sci.* 9, 2015, pp. 614–623.

[35] P. Heřman and D. Zapletal, Modeling of Emission and Absorption Spectra of LH2 Complex (B850 and B800 Ring) – Full Hamiltonian Model, *Int. J. Math. Comp. Sim.* 10, 2016, pp. 208–217.

[36] P. Heřman and D. Zapletal, B$-\alpha$/B$-\beta$ Ring from Photosynthetic Complex LH4, Modeling of Absorption and Fluorescence Spectra, *Int. J. Math. Comp. Sim.* 10, 2016, pp. 332–344.

[37] P. Heřman and D. Zapletal, B850 Ring from Photosynthetic Complex LH2 - Comparison of Different Static Disorder Types, *Int. J. Math. Comp. Sim.* 10, 2016, pp. 361–369.

[38] P. Heřman and D. Zapletal, Fluctuations of Bacteriochlorophylls Positions in B850 Ring from Photosynthetic Complex LH2 *Int. J. Math. Comp. Sim.* 10, 2016, pp. 381–389.

[39] P. Heřman, I. Barvík and D. Zapletal, Energetic disorder and exciton states of individual molecular rings, *J. Lumin.* 119–120, 2006, pp. 496–503.

[40] C. Hofmann, T. J. Aartsma and J. Kőhler, Energetic disorder and the B850–exciton states of individual light–harvesting 2 complexes from Rhodopseudomonas acidophila, *Chem. Phys. Lett.* 395, 2004, pp. 373–378.